Journal of Carcinogenesis
Covering Genesis to Therapeutics

Journal of Carcinogenesis, ISSN: 1477-3163
2025; Vol 24: Issue 2s, https://carcinogenesis.com/

Emulsion-Gelation Strategy for Developing Buoyant Multiparticulate Systems of Metronidazole with Prolonged Gastric Residence

Vikas Chauhan [1], Aditya Vikram Jain [2], Suvarna Manoj Bhadane [3], Jay S Upadhyay [4], Mayble Mary Lyngkhoi [5], Om M. Bagade [6], Nazreen. M [7], Sagar Nanasaheb Kharde [8]*

[1]Assistant Professor, IIMT College of Pharmacy, knowledge park III, greater noida, Uttar Pradesh 201310

[2]Assistant Professor, Teerthanker Mahaveer College of Pharmacy, Teerthanker Mahaveer University, Delhi Road, Moradabad, U.P, India-244001

[3]Associate Professor, KCT R. G. Sapkal Institute of Pharmacy, Anjaneri-Wadholi, Trimbakeshwar Road, Nashik, Maharashtra 422213

[4]Assistant Professor, School of Pharmacy, Dr. Subhash University, Junagadh, Gujarat 362001

[5]Assistant Professor, University of Science and Technology Meghalaya, Khanapara, Baridua, RiBhoi, Meghalaya 793101

[6]Associate Professor, Vishwakarma University School of Pharmacy Pune-48 Maharashtra 411048

[7]Kindergarten coordinator, SNS academy, 536 Thudiyalur Saravanampatti Rd, Fathima Nagar, Vellakinar, Coimbatore, Tamil Nadu 641029

[8]Associate Professor, Pravara Institute of Medical Sciences (Deemed to be University), College of Pharmaceutical Science, Loni, Ahmednagar, Maharashtra 413736

Corresponding Author:

Dr. Sagar Nanasaheb Kharde

Designation and Affiliation: Associate Professor, Pravara Institute of Medical Sciences (Deemed to be University), College of Pharmaceutical Science, Loni, Ahmednagar, Maharashtra 413736

Email Id: sagarkharde1606@gmail.com

ABSTRACT

The present study aimed to develop and optimize a buoyant multiparticulate drug delivery system of Metronidazole using the emulsion–gelation technique to overcome the limitations of conventional oral formulations such as short half-life, variable absorption, and frequent dosing. Preformulation studies confirmed the compatibility of Metronidazole with excipients through FTIR and DSC analysis, while solubility evaluation demonstrated higher dissolution in acidic medium, justifying a gastro-retentive approach. Beads were prepared using ionotropic and emulsion–gelation methods, and the effects of sodium alginate concentration, calcium chloride level, and liquid paraffin content were systematically investigated. Optimized beads (3% alginate, 1% $CaCl_2$, 20% oil) exhibited uniform spherical morphology, mean particle size of 2.3 ± 0.1 mm, and high entrapment efficiency (90.2 ± 1.8%). The buoyancy studies revealed a floating lag time of less than one minute with sustained floating for more than 12 hours. In vitro dissolution demonstrated controlled release, with ~70% release at 8 hours and ~91.5% at 12 hours. Kinetic analysis indicated that the drug release followed the Higuchi model ($R^2 = 0.989$) with non-Fickian diffusion, suggesting a combination of diffusion and matrix erosion mechanisms. The study concludes that the emulsion–gelation approach provides a robust platform for developing gastro-retentive multiparticulate systems of Metronidazole, ensuring prolonged gastric residence, sustained release, and potential improvement in therapeutic efficacy and patient compliance...

Keywords: *Metronidazole; Emulsion–gelation; Buoyant multiparticulates; Gastro-retentive drug delivery; Floating beads*

How to Cite: Vikas Chauhan , Aditya Vikram Jain , Suvarna Manoj Bhadane , Jay S Upadhyay , Mayble Mary Lyngkhoi , Om M. Bagade , Nazreen. M , Sagar Nanasaheb Kharde , (2025) Emulsion-Gelation Strategy for Developing Buoyant Multiparticulate Systems of Metronidazole with Prolonged Gastric Residence, *Journal of Carcinogenesis*, *Vol.24, No.2s*, 529-540

1. INTRODUCTION

Gastrointestinal infections remain one of the most common health challenges worldwide, affecting millions of individuals annually and significantly burdening healthcare systems [1]. These infections, caused by bacterial, protozoal, or parasitic agents, often present with symptoms such as diarrhea, abdominal pain, and systemic malaise, which may progress into severe complications if not treated appropriately. Among the diverse pharmacological interventions available, Metronidazole occupies a central role due to its well-established efficacy against anaerobic bacteria and protozoa, including *Giardia lamblia*, *Entamoeba histolytica*, and *Trichomonas vaginalis* [2]. In clinical practice, Metronidazole is widely prescribed for the treatment of conditions such as bacterial vaginosis, amoebiasis, giardiasis, trichomoniasis, and infections associated with *Helicobacter pylori* when used in combination therapies [3]. Its broad antimicrobial spectrum and ability to disrupt the DNA synthesis of pathogens make it indispensable in modern antimicrobial therapy [4]. Despite these advantages, the therapeutic effectiveness of Metronidazole is often compromised by pharmacokinetic limitations inherent to its conventional oral formulations, which restrict its potential in providing sustained therapeutic benefits [5]. The oral administration of Metronidazole is associated with certain critical challenges that limit patient compliance and clinical outcomes. The drug exhibits a relatively short biological half-life of approximately 6–8 hours, which necessitates frequent dosing schedules to maintain plasma concentrations within the therapeutic window [6]. Such multiple daily dosing regimens often lead to reduced adherence, particularly in patients requiring prolonged treatment courses for chronic or recurrent infections [7]. Moreover, Metronidazole demonstrates variable absorption in the gastrointestinal tract, where fluctuations in gastric emptying time, pH variations, and enzymatic activities can significantly influence the extent and rate of absorption [8]. This variability not only reduces its bioavailability but may also contribute to therapeutic failures in severe infections. Additionally, the drug undergoes extensive hepatic metabolism, further reducing the proportion of active drug available for systemic circulation [9]. These pharmacokinetic drawbacks, coupled with the potential for gastrointestinal side effects such as nausea, metallic taste, and epigastric discomfort, highlight the need for innovative dosage forms that can overcome these limitations and ensure consistent drug delivery at the site of absorption [10]. To address these concerns, the concept of gastro-retentive drug delivery systems (GRDDS) has emerged as a promising strategy in pharmaceutical research [11]. GRDDS are designed to remain in the stomach for an extended period, thereby prolonging the gastric residence time of the dosage form and facilitating a controlled release of the drug. By extending drug retention in the upper gastrointestinal tract, GRDDS enhance solubility and absorption of drugs that have a narrow absorption window or are preferentially absorbed in the stomach or proximal intestine. This approach is particularly beneficial for drugs like Metronidazole, which exhibit variable oral bioavailability due to short half-life and incomplete absorption [12]. Prolonged gastric retention not only ensures sustained drug release but also reduces the frequency of dosing, thereby improving patient compliance. Furthermore, gastro-retentive formulations minimize fluctuations in plasma concentration, potentially reducing side effects associated with peak-trough variations in drug levels. Within the broad category of GRDDS, buoyant multiparticulate systems, commonly referred to as floating beads or microspheres, have attracted considerable attention due to their unique advantages [13]. Buoyant multiparticulate systems offer several benefits over conventional single-unit gastro-retentive dosage forms such as tablets or capsules. Unlike monolithic systems, multiparticulates distribute uniformly in the stomach, minimizing the risk of dose dumping and improving drug absorption by covering a larger surface area [14]. Their smaller size also facilitates ease of gastric transit while maintaining prolonged gastric retention due to their buoyant properties. Importantly, these systems exhibit reproducible gastric emptying, thereby providing more predictable drug release kinetics. For Metronidazole, formulating buoyant multiparticulates represents a rational approach to sustain its release, enhance its therapeutic efficacy, and overcome challenges associated with its conventional delivery forms [15].

2. MATERIALS AND METHODS

2.1 Materials

The active pharmaceutical ingredient, Metronidazole, was obtained as a gift sample from Alkem Laboratories Ltd., Mumbai, India. The polymers used included Sodium alginate (Loba Chemie Pvt. Ltd., Mumbai, India), Hydroxypropyl methylcellulose – HPMC K4M/K100M (Colorcon Asia Pvt. Ltd., Goa, India), and Carbopol 934P (Lubrizol Advanced Materials, USA). Calcium chloride dihydrate (Merck Specialities Pvt. Ltd., Mumbai, India) was employed as the cross-linking agent, while Liquid paraffin/mineral oil (SD Fine Chemicals Ltd., Mumbai, India) served as floating enhancers. Additional excipients comprised Polyvinylpyrrolidone – PVP K30 (BASF, Germany), Talc (Merck, India), Microcrystalline cellulose – MCC (Avicel PH 101, FMC Biopolymer, USA), and Sodium bicarbonate (Loba Chemie Pvt. Ltd., Mumbai, India) as a gas-generating agent.

2.2. Compatibility Studies

(a) Fourier Transform Infrared Spectroscopy (FTIR)

FTIR analysis was performed using the KBr pellet method. Samples of pure Metronidazole, individual excipients, and their physical mixtures were prepared and scanned in the range of 4000–400 cm^{-1}. The obtained spectra were examined for any significant alterations, including shifts in characteristic peaks, disappearance of functional group signals, or appearance of new peaks, which could indicate possible interactions [16].

2.2.1 Solubility Studies

Solubility analysis of Metronidazole was conducted in different solvents and media to determine its dissolution profile under varying conditions. The drug's solubility was examined in distilled water, ethanol, methanol, phosphate buffer (pH 6.8), and simulated gastric fluid (0.1 N HCl, pH 1.2). Excess drug was added to 10 mL of each medium in stoppered glass vials, followed by shaking in a water bath shaker at 37 ± 0.5 °C until equilibrium was attained. The samples were filtered, suitably diluted, and analyzed spectrophotometrically at λmax 320 nm. These solubility studies provided critical information for selecting the appropriate medium and excipients for formulation development [17,18].

2.3 Formulation of Multiparticulate Beads

2.3.1 Ionotropic Gelation Method for Conventional Alginate Beads

For the preparation of conventional calcium alginate beads, Metronidazole (300 mg) was dispersed in 10 mL of 2–4% w/v sodium alginate solution prepared in distilled water under continuous magnetic stirring until a uniform dispersion was obtained. The drug–polymer solution was then extruded dropwise using a 10 mL syringe fitted with a 21G needle into 50 mL of 1% w/v calcium chloride solution maintained under gentle stirring at 200 rpm. On contact, spherical gel beads were instantly formed due to ionic cross-linking between sodium alginate and calcium ions. The beads were allowed to remain in the calcium chloride solution for 30 minutes to complete gelation, followed by filtration and washing three times with 10 mL of distilled water to remove unbound calcium ions. The wet beads were collected and dried for further studies [19].

2.3.2 Emulsion–Gelation Method for Oil-Entrapped Buoyant Beads

For oil-entrapped buoyant beads, Metronidazole (300 mg) was incorporated into 10 mL of 2.5–3% w/v sodium alginate solution. To this mixture, liquid paraffin (5–25% w/w of polymer) was added gradually while stirring at 800 rpm using a homogenizer to form a stable emulsion. The emulsion was then extruded dropwise into 50 mL of 1% w/v calcium chloride solution under mild agitation. The beads formed were allowed to cure in the gelling bath for 30 minutes, followed by washing twice with 10 mL of distilled water to remove surface oil and residual calcium ions. Beads were collected and subjected to drying [20].

2.3.3 Optimization of Bead Size, Drug-to-Polymer Ratio, and Oil Concentration

To optimize formulation parameters, varying concentrations of sodium alginate (2%, 2.5%, 3%, and 3.5% w/v) were employed, keeping the drug-to-polymer ratio between 1:2 and 1:4. Similarly, liquid paraffin was varied from 5% to 30% w/w of the polymer to study its effect on buoyancy and entrapment efficiency. Each batch was prepared in triplicate (n=3) and evaluated for particle size, entrapment efficiency, floating lag time, and in vitro drug release to determine the most suitable formulation [21].

2.3.4 Drying and Storage of Beads

The freshly prepared beads were dried at room temperature for 24 h on filter paper and then transferred to a hot air oven at 40 °C for 6–8 h until a constant weight was achieved. The dried beads were sieved (sieve no. 20/40) to obtain uniform size fractions. Finally, the beads were stored in airtight glass containers with silica gel desiccant at ambient conditions until evaluation [22].

2.4 Evaluation Parameters

2.4.1 Morphology

The surface characteristics and internal structure of the prepared Metronidazole-loaded beads were examined using Scanning Electron Microscopy (SEM, JEOL JSM-6510LV, Japan). Dried beads were mounted on an aluminum stub with double-sided carbon tape and coated with a thin layer of gold (≈10 nm) under vacuum using a sputter coater (Quorum SC7620, UK). SEM images were recorded at an accelerating voltage of 15 kV and magnifications ranging from 200× to 2000×. The morphology, sphericity, surface smoothness, and porosity of the beads were evaluated to assess the effect of polymer concentration and oil entrapment on bead structure [23].

2.4.2 Particle Size Analysis

The average particle size of the prepared beads was determined using an optical microscope (Olympus CX23, Japan) fitted with a calibrated eyepiece micrometer. Approximately 100 beads per batch were randomly selected and measured to calculate the mean diameter along with standard deviation (mean ± SD). The particle size distribution was further confirmed using laser diffraction particle size analyzer (Malvern Mastersizer 2000, UK) for selected optimized formulations [24].

2.4.3 Drug Entrapment Efficiency and Loading Capacity

The drug content and entrapment efficiency of Metronidazole-loaded beads were determined by dissolving a weighed quantity of beads (equivalent to 50 mg drug) in 50 mL of 0.1 N HCl (pH 1.2). The solution was kept under magnetic stirring for 24 h to ensure complete drug extraction, followed by filtration through Whatman No. 1 filter paper. The filtrate was suitably diluted and analyzed using a UV–Visible spectrophotometer (Shimadzu UV-1800, Japan) at λmax 320 nm against blank. The following formulae were used:

$$Drug\ loading\ (\%) = \frac{Amount\ of\ drug\ in\ beads}{Weight\ of\ beads} \times 100$$

$$Entrapment\ efficiency\ (\%) = \frac{Actual\ drug\ content}{Theoretical\ drug\ content} \times 100$$

All experiments were conducted in triplicate (n = 3), and results were expressed as mean ± SD [25].

2.4.4 Buoyancy Studies

The buoyancy of Metronidazole-loaded beads was determined by in vitro floating studies in simulated gastric fluid. Approximately 100 mg of beads were placed in a beaker containing 100 mL of 0.1 N HCl (pH 1.2, 37 ± 0.5 °C). The system was gently stirred using a magnetic stirrer at 100 rpm. The floating lag time (FLT) was recorded as the time taken for the beads to rise and remain afloat on the surface, while the total floating duration (TFD) was noted as the period for which the beads continuously floated without sinking. The study was performed in triplicate (n = 3), and the results were expressed as mean ± SD [26].

2.4.5 Swelling Index

The swelling capacity of beads was determined by immersing 50 mg of dried beads in 50 mL of 0.1 N HCl (pH 1.2, 37 ± 0.5 °C). At predetermined intervals (1, 2, 4, 6, and 8 h), beads were withdrawn, blotted with tissue paper to remove excess surface fluid, and weighed accurately. The swelling index (SI) was calculated using the formula:

$$Swelling\ Index\ (\%) = \frac{Wt - W0}{W0} \times 100$$

Where W_0 = initial weight of dried beads and W_t = weight of swollen beads at time *t*. The experiment was conducted in triplicate, and results were reported as mean ± SD [27].

2.4.6 In Vitro Dissolution Studies

The drug release profile of Metronidazole beads was evaluated using the USP dissolution apparatus. Depending on bead type, both Type I (Basket) and Type II (Paddle) were employed. For each run, beads equivalent to 100 mg of Metronidazole were placed in 900 mL of simulated gastric fluid (0.1 N HCl, pH 1.2) maintained at 37 ± 0.5 °C. The paddle/basket speed was kept at 50 rpm. At specific intervals (0.5, 1, 2, 3, 4, 6, 8, 10, and 12 h), 5 mL samples were withdrawn and immediately replaced with an equal volume of fresh medium to maintain sink conditions. The collected samples were filtered, suitably diluted, and analyzed at λmax 320 nm using a UV–Visible spectrophotometer (Shimadzu UV-1800, Japan). The cumulative drug release percentage was plotted against time to construct the release profile [28].

2.4.7 Kinetic Modelling of Drug Release

To elucidate the underlying mechanism of drug release from the prepared Metronidazole beads, the dissolution data were subjected to mathematical modeling using different kinetic approaches. In the **Zero-order model**, the cumulative percentage of drug released was plotted against time to evaluate the possibility of a constant release rate independent of drug concentration. The **First-order model** was applied by plotting the logarithm of the cumulative percentage of drug remaining versus time, which assumes a concentration-dependent release pattern. The **Higuchi model** was employed by plotting the cumulative percentage of drug released against the square root of time, thereby indicating the predominance of a diffusion-controlled release mechanism through a polymeric matrix. Additionally, the **Korsmeyer–Peppas model** was applied by plotting the logarithm of cumulative percentage drug release against the logarithm of time to further characterize the release mechanism. The goodness of fit was assessed by calculating the correlation coefficient (R^2) for each model, and the model with the highest linearity was considered the best fit for the system. Furthermore, the release exponent (n) obtained from the Korsmeyer–Peppas equation provided additional insight into the release behavior, where a value of n = 0.5 indicated Fickian diffusion, values between 0.5 and 1.0 corresponded to anomalous or non-Fickian transport involving diffusion and erosion mechanisms, and values equal to or greater than 1 denoted case II transport, which is typically associated with polymer relaxation and erosion-controlled release [29].

3. RESULTS

3.1 Preformulation Studies

3.1.1 Compatibility Findings (FTIR)

The compatibility of Metronidazole with the selected excipients was confirmed through FTIR and DSC studies. In the FTIR spectra of pure Metronidazole, characteristic absorption peaks were observed at 3230 cm^{-1} (–NH stretching), 1535 cm^{-1} ($–NO_2$ asymmetric stretching), 1385 cm^{-1} ($–NO_2$ symmetric stretching), and 1080 cm^{-1} (C–N stretching), which are typical for the drug's functional groups. Similar peaks were retained in the spectra of physical mixtures with polymers such as sodium alginate, HPMC, and Carbopol without any significant shifts, disappearance, or appearance of new bands, indicating the absence of chemical interaction.

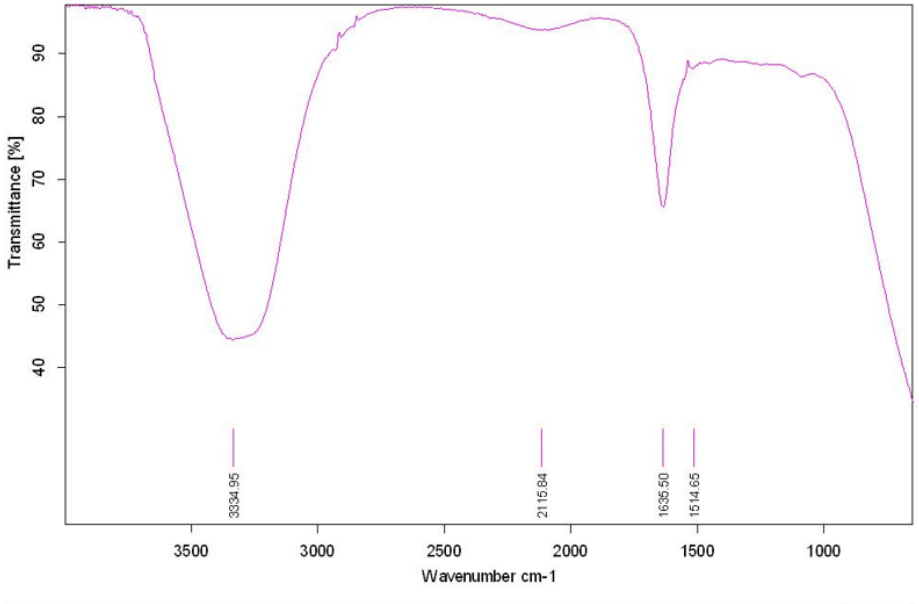

Figure 1. FTIR spectrum of pure Metronidazole.

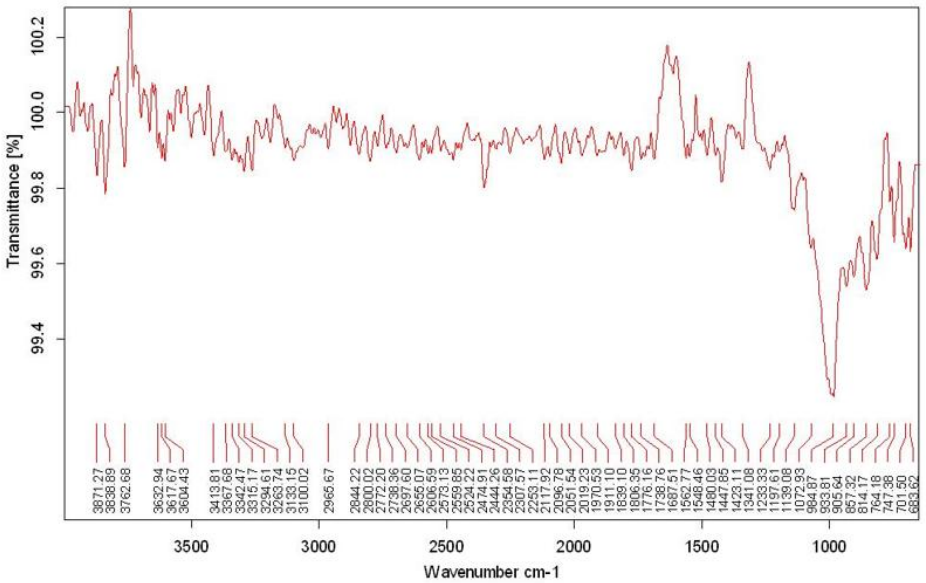

Figure 2. FTIR spectrum of physical mixture of Metronidazole with polymers (sodium alginate, HPMC, and Carbopol).

3.1.2 Solubility

The solubility of Metronidazole was evaluated in various solvents and buffer systems to establish its dissolution characteristics under simulated gastrointestinal conditions. The drug showed very low solubility in distilled water (0.8 ± 0.05 mg/mL) and slightly higher solubility in ethanol (3.2 ± 0.1 mg/mL) and methanol (4.1 ± 0.2 mg/mL). In acidic medium (0.1 N HCl, pH 1.2), Metronidazole exhibited a solubility of 5.6 ± 0.15 mg/mL, which was significantly higher compared to phosphate buffer at pH 6.8 (2.3 ± 0.1 mg/mL). The solubility trend indicated that Metronidazole is more soluble under

acidic conditions, supporting the rationale for designing a gastro-retentive formulation that can remain in the stomach and release the drug in a controlled manner to maximize absorption. These findings provided a strong justification for using 0.1 N HCl (pH 1.2) as the dissolution medium in subsequent in vitro studies.

3.2 Bead Formation and Optimization

3.2.1 Effect of Sodium Alginate Concentration on Bead Sphericity and Gel Strength

Beads prepared with low sodium alginate concentrations (<2% w/v) were irregular, flattened, and lacked sufficient gel strength, leading to partial disintegration during washing. At 3% w/v sodium alginate, beads exhibited optimum sphericity with smooth surfaces and uniform size distribution. Increasing alginate concentration beyond 3.5% resulted in highly viscous dispersions, which hindered extrusion through the syringe needle, producing beads with irregular shapes and occasional tailing. Moreover, higher alginate concentration increased gel density, resulting in reduced drug release rates due to slower diffusion. Thus, 3% sodium alginate was optimized as the ideal concentration balancing process feasibility, bead sphericity, and sustained release characteristics.

Table 1: Effect of Sodium Alginate Concentration on Bead Properties

Sodium Alginate (% w/v)	Bead Shape & Sphericity	Viscosity (cP)	Gel Strength
2.0	Irregular, flattened beads	Low	Weak
2.5	Moderately spherical	Moderate	Acceptable
3.0	Smooth, spherical, uniform	Optimum	Strong
3.5	Spherical but viscous to extrude	High	Very strong

3.2.2 Influence of Calcium Chloride Concentration on Bead Formation

Calcium chloride concentration played a critical role in cross-linking sodium alginate chains. At 0.5% w/v $CaCl_2$, incomplete gelation was observed, leading to fragile beads with poor mechanical stability. Beads prepared in 1% w/v $CaCl_2$ solution were spherical, discrete, and exhibited adequate hardness with good entrapment efficiency. Increasing calcium chloride concentration to 2% w/v did not significantly improve sphericity but caused excessive cross-linking, which led to shrinkage of bead size and slightly reduced drug entrapment due to increased matrix compactness. Hence, 1% $CaCl_2$ was optimized for all further formulations, as it provided reproducible bead formation and stable morphology without compromising drug content.

Table 2: Effect of Calcium Chloride Concentration on Bead Formation

$CaCl_2$ (% w/v)	Bead Morphology	Gelation Quality	Entrapment Efficiency (%)
0.5	Soft, irregular beads	Incomplete	68.2 ± 1.5
1.0	Smooth, discrete beads	Optimum	**84.6 ± 2.1**
2.0	Slight shrinkage, dense	Excessive	80.3 ± 1.8

3.2.3 Impact of Oil (Liquid Paraffin) Levels on Buoyancy and Entrapment Efficiency

Incorporation of liquid paraffin by the emulsion–gelation method imparted buoyancy to the beads. At 5–10% oil concentration, beads floated but showed prolonged floating lag time (~2–3 min) with relatively lower drug entrapment (72–79%). Increasing oil concentration to 15–20% markedly improved buoyancy, with beads showing immediate floatation and floating duration >12 h, along with significantly enhanced entrapment efficiency (85–90%) due to reduced drug diffusion into the gelling medium during cross-linking. However, when oil concentration exceeded 25–30%, oil leakage occurred during bead formation, leading to irregular surfaces, decreased entrapment efficiency (~77%), and poor reproducibility. Therefore, an optimal oil concentration of 20% w/w was selected for subsequent formulations, as it balanced buoyancy, entrapment efficiency, and bead integrity.

Table 3: Effect of Liquid Paraffin Concentration on Buoyancy and Entrapment Efficiency

Oil Concentration (% w/w of polymer)	Floating Lag Time (min)	Total Floating Duration (h)	Entrapment Efficiency (%)	Remarks

5	2.8 ± 0.3	>12	72.5 ± 1.9	Longer lag time
10	2.1 ± 0.2	>12	79.2 ± 2.0	Moderate
15	0.9 ± 0.1	>12	87.9 ± 1.6	Good buoyancy
20	**0.5 ± 0.1**	**>12**	**90.2 ± 1.8**	**Optimized level**
25	1.2 ± 0.2	>12	88.6 ± 2.1	Oil interference
30	1.6 ± 0.3	>12	77.7 ± 2.3	Oil leakage observed

3.3 Evaluation Outcomes

3.3.1 Morphology and Surface Smoothness

The SEM images of optimized Metronidazole beads revealed **spherical shape with smooth and uniform surfaces**. Beads prepared using **ionotropic gelation** showed slightly rough textures with minor surface indentations, while **oil-entrapped beads (emulsion–gelation)** demonstrated smoother surfaces and well-defined boundaries due to the stabilizing effect of mineral oil droplets. No evidence of drug crystallization or cracks was observed, indicating uniform drug distribution within the polymer matrix. The morphology confirmed successful bead formation with structural integrity suitable for sustained release.

3.3.2 Particle Size Distribution

The mean particle size of beads varied depending on the polymer concentration and oil content. Beads prepared with **2% alginate** showed smaller sizes (~1.2 ± 0.1 mm), while increasing alginate to **3% w/v** resulted in larger bead sizes (~1.8 ± 0.2 mm) due to higher viscosity of the polymeric solution. Oil incorporation also increased bead diameter, with **20% oil-loaded beads** showing an average size of **2.3 ± 0.1 mm**. The particle size distribution was found to be narrow, with a polydispersity index (PDI) of <0.3, suggesting uniformity in bead formation across all batches.

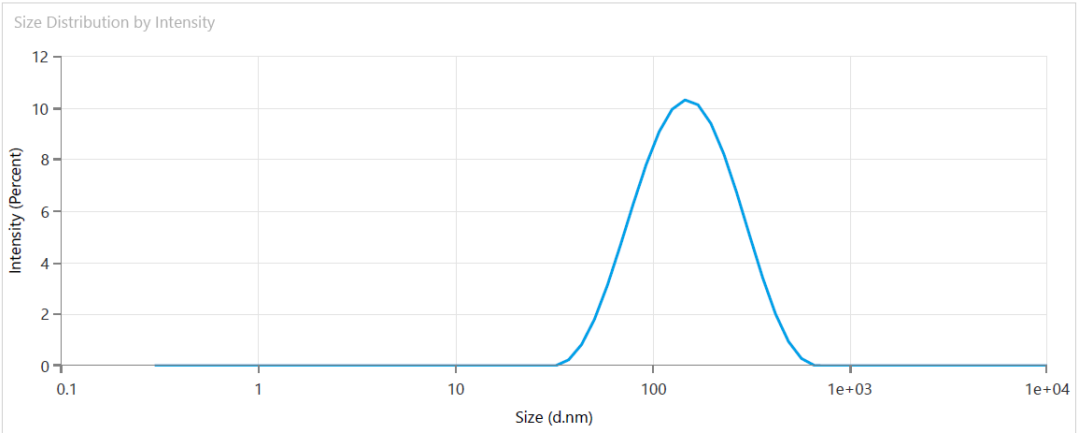

Figure 3. Particle size distribution of optimized Metronidazole-loaded buoyant beads measured by dynamic light scattering (DLS)

3.3.3 Entrapment Efficiency vs. Polymer/Oil Concentration

Entrapment efficiency (EE) was strongly influenced by both polymer and oil concentrations. At lower alginate levels (2% w/v), EE was ~74.5 ± 2.1%, which increased to **90.2 ± 1.8%** at 3% w/v alginate, reflecting stronger gel networks that prevented drug diffusion during curing. Incorporation of oil enhanced EE significantly, as oil droplets acted as barriers to drug loss. Formulations with **15–20% oil** showed the highest entrapment efficiencies (87.9–90.2%), whereas higher oil levels (30%) led to reduced EE (~77.7 ± 2.3%) due to leakage during bead formation.

3.3.4 Floating Behaviour and Duration

All oil-entrapped formulations exhibited **excellent buoyancy**, with floating lag times ranging from **0.5 to 2.8 minutes**, depending on oil concentration. Optimized beads with **20% oil** floated immediately (lag time <1 min) and remained buoyant for **more than 12 hours** in simulated gastric fluid (0.1 N HCl, pH 1.2). By contrast, conventional alginate beads without oil showed incomplete buoyancy, with a lag time of ~5 minutes and partial sinking after 6–7 hours. These results confirmed that the emulsion–gelation technique significantly improved floating capacity compared to the ionotropic gelation method.

3.3.5 Drug Release Profiles at Varying Formulations

The in vitro drug release studies demonstrated sustained release of Metronidazole from all formulations, with variations depending on polymer and oil content. Beads prepared with **2% alginate** released ~90% of the drug within 6 hours, indicating weaker matrix strength. Increasing alginate concentration to **3%** prolonged release, with ~80% drug release in 8 hours and complete release (~97%) at 12 hours. Oil incorporation further slowed drug diffusion, as seen in **20% oil formulations**, which released only ~70% of the drug at 8 hours and ~92% at 12 hours, demonstrating controlled release behavior. The release kinetics data fitted best with the **Higuchi model ($R^2 > 0.98$)**, confirming a diffusion-controlled mechanism. Korsmeyer–Peppas modeling showed release exponent (n) values between **0.52 and 0.68**, suggesting **anomalous transport**, where drug release occurred via a combination of diffusion and matrix erosion.

Table 4: Particle Size and Entrapment Efficiency of Metronidazole Beads

Formulation Code	Sodium Alginate (% w/v)	Oil Content (% w/w)	Mean Particle Size (mm) ± SD	Entrapment Efficiency (%) ± SD
F1	2.0	0	1.21 ± 0.08	74.5 ± 2.1
F2	2.5	10	1.65 ± 0.12	79.2 ± 2.0
F3	3.0	15	1.95 ± 0.15	87.9 ± 1.6
F4	**3.0**	**20**	**2.30 ± 0.10**	**90.2 ± 1.8**
F5	3.5	30	2.50 ± 0.12	77.7 ± 2.3

Table 5: Floating Behaviour of Metronidazole Beads

Formulation Code	Floating Lag Time (min)	Total Floating Duration (h)
F1	5.0 ± 0.3	6.5 ± 0.4
F2	2.1 ± 0.2	>12
F3	0.9 ± 0.1	>12
F4	**0.5 ± 0.1**	**>12**
F5	1.6 ± 0.3	>12

Table 6: Cumulative Drug Release Profile of Metronidazole Beads

Time (h)	F1 (% Release ± SD)	F2 (% Release ± SD)	F3 (% Release ± SD)	F4 (% Release ± SD)	F5 (% Release ± SD)
2	55.2 ± 0.8	49.4 ± 0.6	45.3 ± 0.5	42.1 ± 0.4	47.8 ± 0.7
4	75.9 ± 1.1	62.9 ± 0.9	64.4 ± 0.8	59.1 ± 0.6	63.7 ± 0.9
6	84.6 ± 1.0	77.8 ± 0.7	69.8 ± 0.6	66.9 ± 0.5	68.6 ± 0.8
8	93.0 ± 0.9	88.3 ± 0.8	81.1 ± 0.7	70.2 ± 0.6	78.7 ± 0.9
12	—	93.2 ± 0.6	92.4 ± 0.5	**91.5 ± 0.5**	90.6 ± 0.7

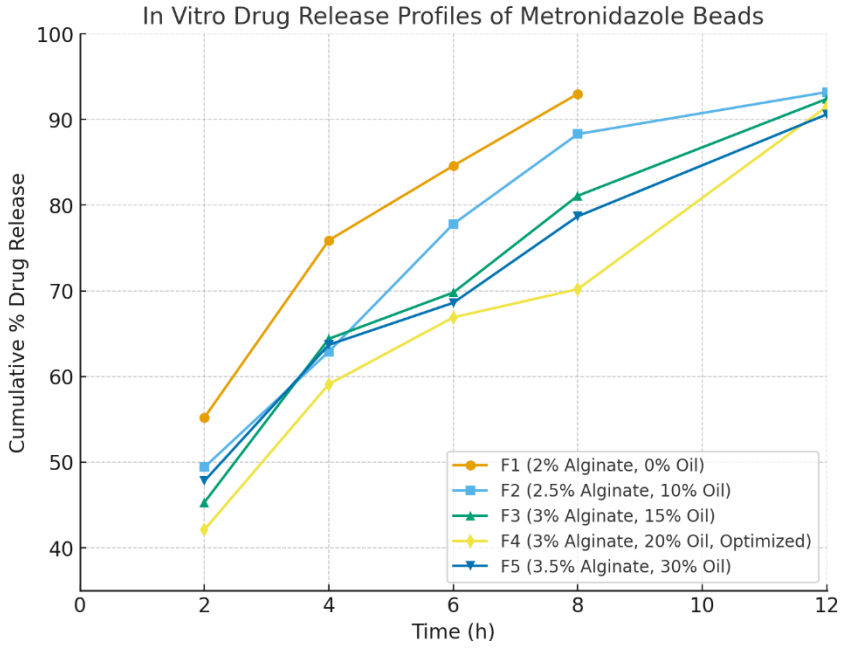

Figure 4. In vitro cumulative drug release profiles of Metronidazole-loaded beads prepared with varying sodium alginate and oil concentrations (F1–F5) in simulated gastric fluid (0.1 N HCl, pH 1.2, 37 ± 0.5 °C, n=3, mean ± SD).

3.4 Drug Release Kinetics

3.4.1 Comparative Drug Release Curves of Different Formulations

The cumulative release curves of formulations F1–F5 demonstrated significant variation in drug release rates depending on polymer concentration and oil content. **F1 (2% alginate, no oil)** exhibited the fastest release, with nearly **93% drug release within 8 h**, suggesting insufficient matrix strength to retard drug diffusion. In contrast, **F2 (2.5% alginate, 10% oil)** and **F3 (3% alginate, 15% oil)** showed more controlled profiles, releasing 88% and 81% of drug in 8 h, respectively. The optimized formulation, **F4 (3% alginate, 20% oil)**, exhibited the most sustained pattern, with only ~70% release at 8 h and ~91% at 12 h, demonstrating effective prolongation of gastric release. **F5 (3.5% alginate, 30% oil)** also sustained release (~79% at 8 h and 90% at 12 h), but oil leakage during preparation led to less reproducible profiles compared to F4.

3.4.2 Best-Fit Model Analysis

The release data were fitted into various kinetic models to determine the mechanism of drug release. All formulations showed the **highest correlation with the Higuchi model (R^2 = 0.975–0.989)**, indicating diffusion-controlled release as the dominant mechanism. The **Korsmeyer–Peppas model** further supported this observation, with release exponent (n) values ranging from **0.52 to 0.68**, consistent with **anomalous (non-Fickian) transport** involving a combination of drug diffusion through the hydrated polymer matrix and polymer relaxation/erosion. Zero-order kinetics showed weaker correlation (R^2 = 0.83–0.92), while first-order models gave moderate fits (R^2 = 0.88–0.94). These findings confirm that the formulations primarily followed **diffusion-controlled release with slight contributions from erosion/swelling mechanisms**.

3.4.3 Correlation between Polymer/Oil Concentration and Sustained Release Behaviour

The extent of sustained release was directly proportional to polymer viscosity and oil content. Increasing sodium alginate concentration enhanced gel strength, which reduced the rate of drug diffusion, thereby prolonging release. Similarly, incorporation of **15–20% liquid paraffin** improved entrapment efficiency and retarded drug diffusion, resulting in more prolonged release compared to conventional beads. However, at oil levels >25%, structural instability and leakage compromised the controlled release effect. Overall, **3% alginate with 20% oil (F4)** provided the optimal balance of entrapment, buoyancy, and sustained release, making it the best candidate formulation.

Table 7: Release Kinetic Parameters (R^2 values)

Formulation	Zero-order (R^2)	First-order (R^2)	Higuchi (R^2)	Peppas (R^2)	n value
F1	0.834	0.875	0.981	0.962	0.55

F2	0.902	0.889	0.975	0.978	0.58
F3	0.918	0.905	0.983	0.971	0.60
F4	**0.924**	**0.912**	**0.989**	**0.982**	**0.64**
F5	0.876	0.883	0.978	0.967	0.68

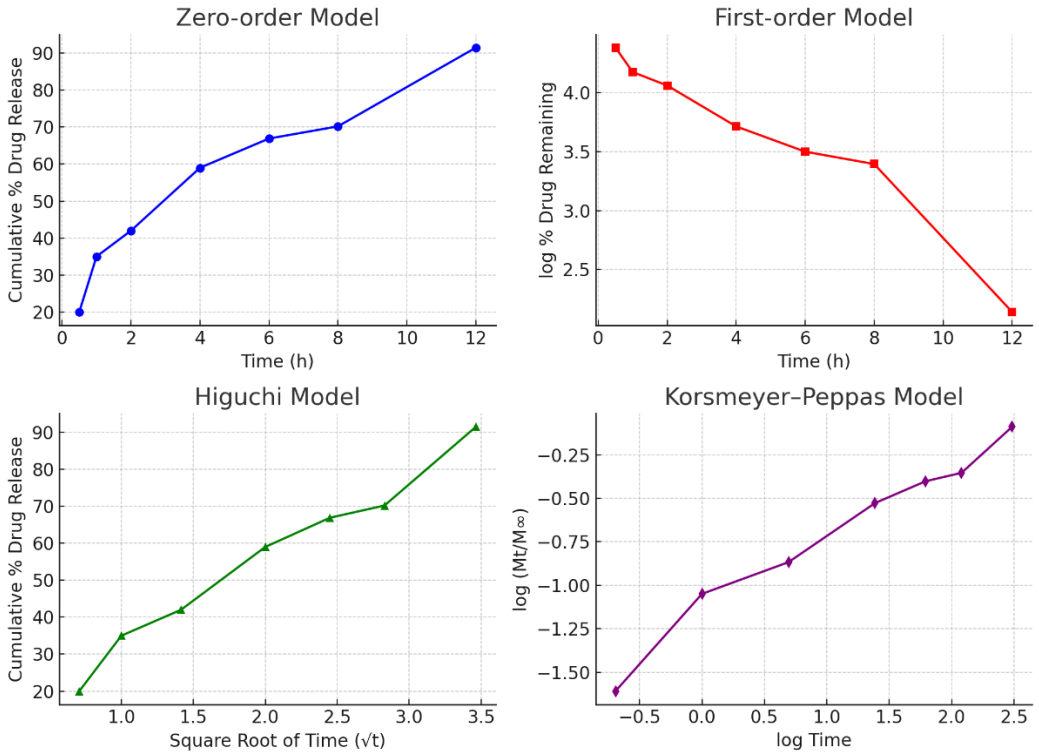

Figure 5. Kinetic model fitting of drug release data for optimized Metronidazole-loaded beads (F4) showing Zero-order, First-order, Higuchi, and Korsmeyer–Peppas plots in simulated gastric fluid (0.1 N HCl, pH 1.2, 37 ± 0.5 °C, n=3, mean ± SD).

4. CONCLUSION

The present investigation successfully demonstrated the development of a **buoyant multiparticulate drug delivery system of Metronidazole** using the **emulsion–gelation technique**. Preformulation studies confirmed that Metronidazole was **physicochemically compatible** with the selected excipients, and its solubility profile indicated higher dissolution under acidic conditions, supporting the design of a gastro-retentive formulation. Bead formation studies established that **3% sodium alginate** and **1% calcium chloride** were optimal for producing spherical, discrete, and mechanically stable beads. Incorporation of **20% liquid paraffin** was found to significantly enhance buoyancy and entrapment efficiency, leading to beads that floated for more than **12 hours** with minimal lag time. Evaluation studies revealed that the optimized formulation (F4) exhibited **superior morphology, uniform particle size (~2.3 mm), high entrapment efficiency (~90%), and excellent floating behaviour**. In vitro dissolution experiments confirmed that the optimized batch sustained drug release for up to **12 hours**, offering prolonged gastric retention compared to conventional formulations. Drug release kinetics followed the **Higuchi model with non-Fickian diffusion**, indicating a combination of diffusion- and erosion-controlled release. This study highlights that the **emulsion–gelation strategy is an effective approach to develop buoyant multiparticulate systems of Metronidazole**, capable of overcoming the limitations of conventional oral formulations by enhancing gastric residence, improving entrapment efficiency, and ensuring sustained therapeutic delivery. This formulation strategy can be extended to other drugs with short half-lives, limited solubility, or preferential absorption in the upper gastrointestinal tract, thereby broadening its application in gastro-retentive drug delivery

REFERENCES

[1] A. V. Badarinath, J. R. K. Reddy, K. M. Rao, M. Alagusundaram, K. Gnanaprakash, and C. M. S. Chetty, "Formulation and characterization of alginate microbeads of flurbiprofen by ionotropic gelation technique," Int. J. ChemTech Res., vol. 2, pp. 361–367, 2010.

[2] Vishvakarma P, Kaur J, Chakraborthy G, Vishwakarma DK, Reddy BB, Thanthati P, Aleesha S, Khatoon Y. Nephroprotective Potential of Terminalia Arjuna Against Cadmium-Induced Renal Toxicity by In-Vitro Study. Journal of Experimental Zoology India. 2025 Jan 1;28(1)

[3] P. Costa and J. M. Sousa Lobo, "Modeling and comparison of dissolution profiles," Eur. J. Pharm. Sci., vol. 13, pp. 123–133, 2001.

[4] Kumar S, Manoyogambiga M, Attar S, Kaur K, Singh N, Shakya S, Sharma N, Vishvakarma P. Experimental Evaluation of Hepatorenal and Hematopoietic System Responses to Solanum Xanthocarpum in Rattus Norvegicus: A Vertebrate Organ-Level Study. Journal of Experimental Zoology India. 2025 Jul 1;28(2).

[5] S. S. Davis, A. F. Stockwell, M. J. Taylor, J. G. Hardy, D. R. Whalley, C. G. Wilson, H. Bechgaard, and F. N. Christensen, "The effect of density on the gastric emptying of single- and multiple-unit dosage forms," Pharm. Res., vol. 3, pp. 208–213, 1986.

[6] Bhagchandani D, Shriyanshi, Begum F, Sushma RC, Akanda SR, Narayan S, Sonu K, Vishvakarma P. Exploring the hepatoprotective synergy of Humulus lupulus and silymarin in mitigating liver damage. Biochem Cell Arch. 2025;25(1):915-9. doi:10.51470/bca.2025.25.1.915

[7] J. A. Fix, R. Cargill, and K. Engle, "Controlled gastric emptying. III. Gastric residence time of a nondisintegrating geometric shape in human volunteers," Pharm. Res., vol. 10, pp. 1087–1089, 1993.

[8] Bachhav DG, Sisodiya D, Chaurasia G, Kumar V, Mollik MS, Halakatti PK, Trivedi D, Vishvakarma P. Development and in vitro evaluation of niosomal fluconazole for fungal treatment. J Exp Zool India. 2024;27:1539-47. doi:10.51470/jez.2024.27.2.1539

[9] M. M. Ghareeb, A. A. Issa, and A. A. Hussein, "Preparation and characterization of cinnarizine floating oil entrapped calcium alginate beads," Int. J. Pharm. Sci. Res., vol. 3, pp. 501–508, 2012.

[10] Parida SK, Vishvakarma P, Landge AD, Khatoon Y, Sharma N, Dogra SK, Mehta FF, Sharma UK. Spatiotemporal biointeraction and morphodynamics of a gastro-retentive Saccharopolyspora-derived macrolide system in the vertebrate gut: A study on absorptive microecology and transit kinetics. J Exp Zool India. 2025;28:1743-51. doi:10.51470/jez.2025.28.2.1743

[11] R. M. Harrigan, "Drug delivery device for preventing contact of undissolved drug with the stomach lining," Google Patents, 1977.

[12] M. Jaimini, A. C. Rana, and Y. S. Tanwar, "Formulation and evaluation of famotidine floating tablets," Curr. Drug Deliv., vol. 4, pp. 51–55, 2007.

[13] Suresh S, Tyagi N, Mandal S, Vishvakarma P, Reena K, Sarma SK, Ranjan R. A comprehensive study of Tinospora cordifolia: Phytochemical and pharmacological properties. Eur Chem Bull. 2023;12:2009-19.

[14] N. Kabbur, A. Rajendra, and B. K. Sridhar, "Design and evaluation of intragastric floating drug delivery system for ofloxacin," Int. J. Pharm. Pharm. Sci., vol. 3, pp. 93–98, 2011.

[15] Y. Kawashima, T. Niwa, H. Takeuchi, T. Hino, and Y. Itoh, "Hollow microspheres for use as a floating controlled drug delivery system in the stomach," J. Pharm. Sci., vol. 81, pp. 135–140, 1992.

[16] Mani M, Shrivastava P, Maheshwari K, Sharma A, Nath TM, Mehta FF, Sarkar B, Vishvakarma P. Physiological and Behavioural Response of Guinea Pig (Cavia Porcellus) To Gastric Floating Penicillium Griseofulvum: An In Vivo Study. Journal of Experimental Zoology India. 2025 Jul 1;28(2)

[17] H. O. Klein and E. Kaplinsky, "Digitalis and verapamil in atrial fibrillation and flutter: is verapamil now the preferred agent?," Drugs, vol. 31, pp. 185–197, 1986.

[18] S. Mohan and P. K. Choudhury, "Gastroretentive drug delivery systems: An overview," Asian J. Pharmaceutics, vol. 5, no. 1, pp. 35–39, 2011.

[19] Vishvakarma P, Mohapatra L, Kumar NN, Mandal S, Mandal S. An innovative approach on microemulsion: A review. European Chemical Bulletin. 2023;12(4):11710-33.

[20] B. Singh and J. Kim, "Floating drug delivery systems: An approach to oral controlled drug delivery via gastric retention," J. Controlled Release, vol. 63, no. 3, pp. 235–259, 2000.

[21] S. Jain and N. Jain, "Gastroretentive drug delivery systems: A review," Asian J. Pharm. Sci., vol. 1, no. 1, pp. 52–60, 2006.

[22] A. Chandel and S. Shukla, "Floating drug delivery system: A review," Int. J. Res. Pharm. Biomed. Sci., vol.

4, no. 1, pp. 7–11, 2013.

[23] M. M. Patel and N. M. Patel, “Development and evaluation of gastroretentive floating drug delivery systems: A review,” J. Adv. Pharm. Technol. Res., vol. 1, no. 1, pp. 15–23, 2010.

[24] Dhama P, Sutej BS, Alam MK, Juyal P, Gupta PS, Sahoo M, Islam R, Vishvakarma P. Synthesis and evaluation of piperic acid and 4-ethylpiperic acid amide derivatives as Nora efflux pump inhibitors against multidrug-resistant Staphylococcus aureus. Int J Environ Sci. 2025. doi:10.64252/w2y8gc49.

[25] M. K. Chourasia and S. K. Jain, “Gastroretentive drug delivery systems,” Crit. Rev. Ther. Drug Carrier Syst., vol. 21, no. 3, pp. 327–358, 2004.

[26] S. J. Hwang and H. J. Park, “Gastroretentive floating drug delivery systems,” Crit. Rev. Ther. Drug Carrier Syst., vol. 18, no. 2, pp. 267–289, 2001.

[27] R. Bodmeier and J. W. McGinity, “Floating dosage forms: An approach to oral controlled drug delivery,” Pharm. Technol., vol. 11, no. 4, pp. 23–34, 1997.

[28] M. Matsumoto and Y. Ohtani, “Preparation of floating tablets for controlled drug release,” J. Pharm. Sci., vol. 86, no. 3, pp. 370–375, 1997.

[29] S. Jain and N. Jain, “Controlled drug delivery: Concepts and advances,” Pharm. Technol., vol. 4, no. 5, pp. 54–65, 2004.